

Synthesis and Characterization of Phosphorescent Cyclometalated Platinum Complexes

Jason Brooks, Yelizaveta Babayan, Sergey Lamansky, Peter I. Djurovich, Irina Tsyba, Robert Bau, and Mark E. Thompson*

Department of Chemistry, University of Southern California, Los Angeles, California 90089-0744

Received February 19, 2002

The synthesis, electrochemistry, and photophysics of a series of square planar Pt(II) complexes are reported. The complexes have the general structure $C^{\wedge}NPt(O^{\wedge}O)$, where $C^{\wedge}N$ is a monoanionic cyclometalating ligand (e.g., 2-phenylpyridyl, 2-(2'-thienyl)pyridyl, 2-(4,6-difluorophenyl)pyridyl, etc.) and $O^{\wedge}O$ is a β -diketonato ligand. Reaction of K_2PtCl_4 with a $HC^{\wedge}N$ ligand precursor forms the chloride-bridged dimer, $C^{\wedge}NPt(\mu-Cl)_2PtC^{\wedge}N$, which is cleaved with β -diketonates such as acetyl acetone (acacH) and dipivaloylmethane (dpmH) to give the corresponding monomeric $C^{\wedge}NPt(O^{\wedge}O)$ complex. The $thpyPt(dpm)$ ($thpy = 2$ -(2'-thienyl)pyridyl) complex has been characterized using X-ray crystallography. The bond lengths and angles for this complex are similar to those of related cyclometalated Pt complexes. There are two independent molecular dimers in the asymmetric unit, with intermolecular spacings of 3.45 and 3.56 Å, consistent with moderate π - π interactions and no evident Pt-Pt interactions. Most of the $C^{\wedge}NPt(O^{\wedge}O)$ complexes display a single reversible reduction wave between -1.9 and -2.6 V (vs Cp_2Fe/Cp_2Fe^+), assigned to largely $C^{\wedge}N$ ligand based reduction, and an irreversible oxidation, assigned to predominantly Pt based oxidation. DFT calculations were carried out on both the ground (singlet) and excited (triplet) states of these complexes. The HOMO levels are a mixture of Pt and ligand orbitals, while the LUMO is predominantly $C^{\wedge}N$ ligand based. The emission characteristics of these complexes are governed by the nature of the organometallic cyclometalating ligand allowing the emission to be tuned throughout the visible spectrum. Twenty-three different $C^{\wedge}N$ ligands have been examined, which gave emission λ_{max} values ranging from 456 to 600 nm. Well-resolved vibronic fine structure is observed in all of the emission spectra (room temperature and 77 K). Strong spin-orbit coupling of the platinum atom allows for the formally forbidden mixing of the 1MLCT with the 3MLCT and $^3\pi-\pi^*$ states. This mixing leads to high emission quantum efficiencies (0.02–0.25) and lifetimes on the order of microseconds for the platinum complexes.

Introduction

A significant research effort has focused on the photo-physical properties of luminescent square planar platinum complexes. These complexes have been investigated as emissive probes for DNA,¹ photosensitizers for hydrogen production,² singlet oxygen sensitizers,³ photooxidants,⁴

liquid crystal optical storage materials,⁵ and photochemical devices for the conversion of light to chemical energy through photoinduced charge separation.⁶ Recently, platinum complexes have been used as luminescent centers in organic light-emitting diodes (OLEDs).^{7,8} A recent breakthrough using phosphorescent luminophores has demonstrated the ability to make highly efficient electroluminescent devices.^{7,9} The strong spin-orbit coupling of the heavy metal atom allows for efficient intersystem crossing (ISC) between

* Author to whom correspondence should be addressed. E-mail: met@usc.edu.

- (1) (a) Peyratout, C. S.; Aldridge, T. K.; Crites, D. K.; McMillin, D. R. *Inorg. Chem.* **1995**, *34*, 4484–4489. (b) Wang, A. H.-J.; Nathans, J.; van der Marel, G. A.; van Boom, J. H.; Rich, A. *Nature (London)* **1978**, *276*, 471–474.
- (2) (a) Houlding, V. H.; Frank, A. J. *Inorg. Chem.* **1985**, *24*, 3664–3668. (b) Maruyama, T.; Yamamoto, T. *J. Phys. Chem. B* **1997**, *101*, 3806–3810.
- (3) Anbalagan, V.; Srivastava, T. S. *J. Photochem. Photobiol., A: Chem.* **1995**, *89*, 113–119.

- (4) Connick, W. B.; Gray, H. B. *J. Am. Chem. Soc.* **1997**, *119*, 11620–11627.
- (5) Buey, J.; Diez, L.; Espinet, P.; Kitzerow, H.-S.; Miguel, J. A. *Chem. Mater.* **1996**, *8*, 2375–2381.
- (6) (a) Hissler, M.; McGarrah, J. E.; Connick, W. B.; Geiger, D. K.; Cummings, S. D.; Eisenberg, R. *Coord. Chem. Rev.* **2000**, *208*, 115–137. (b) McGarrah, J. E.; Kim, Y.-J.; Hissler, M.; Eisenberg, R. *Inorg. Chem.* **2001**, *40*, 4510–4511.

singlet and triplet states, which can lead to a high quantum yield of emission from the triplet state. Thus, OLEDs can be fabricated that utilize all of the electrogenerated singlet and triplet excitons, thereby approaching an internal efficiency of 100%.¹⁰

While the chemistry and photophysics of coordinatively unsaturated square planar platinum complexes have been extensively explored, it is interesting to note that surprisingly few of them are reported to be emissive in room temperature solution.¹¹ Only Pt(II) species chelated with aromatic ligands, such as bipyridine, phenanthroline, 2-phenylpyridine, or similar derivatives, emit in fluid solution from excited states localized in the aromatic π systems. These Pt(II) complexes benefit from having relatively high energy metal centered (MC) or ligand field excited states when compared with, for example, their palladium analogues.¹² For the Pt complexes, the MC states lie at higher energy than the intraligand and MLCT states, a situation advantageous for enhancing luminous efficiency. If the emitting state (either intraligand or MLCT) and MC states lie too close in energy, they can thermally equilibrate, thereby quenching the emission through fast radiationless decay through the MC states. The energy gap between the MC states and lowest energy emitting excited state may be considered to be one of the limiting factors for emission efficiency (i.e., a small energy gap between emitting and MC states leads to poor emission efficiency).¹³ Additionally, open coordination sites of the square planar complex can allow for other deactivating pathways to occur through metal interactions with the environment.¹¹

A number of early studies of these emissive complexes were focused on the photophysics of Pt(II) diimine dithiolate compounds.^{11,14} Since then, similar diimine-based complexes

have been reported with other ancillary ligands, such as acetylide,¹⁵ aryl,¹⁶ and pyrazole.¹⁷ Studies on the photophysical properties of tridentate terpyridine^{13,18} and phenylbipyridine¹⁹ derivatives have also been reported. The nature and energy of the excited state in these complexes varies depending on the ligand.^{14a,17} For the dithiolate and tridentate complexes, the lowest energy excited state has been attributed to either a triplet metal-to-ligand charge transfer state (³MLCT) or a ligand-based state (either a ligand–ligand charge transfer, LLCT, or single ligand centered triplet excited states, ³LC).

Several cyclometalated organometallic platinum complexes, based on $C^{\wedge}N$ aromatic chelate derivatives (e.g., 2-arylpiperidine), have been reported in the literature. Among the most basic and thoroughly studied complexes are those based on 2-phenylpyridine (*ppy*) and 2-(2'-thienyl)pyridine (*thpy*). Examples of these include homoleptic complexes, ($C^{\wedge}N$)₂,²⁰ heteroleptic complexes, ($C^{\wedge}N$)($C^{\wedge}N'$),²¹ and complexes with a single cyclometalating ligand ($C^{\wedge}N$) and a non-cyclometalating, ancillary ligand (LX).²² The strong ligand field influence of the aromatic carbon atom, along with the added stabilization of π donation from the metal into the aromatic ring, helps to make these types of chelates very stable, while concurrently increasing the energy gap of the MC excited states.^{22a} These cyclometalated complexes are known to be strongly emissive and have long luminescent lifetimes (microseconds) in fluid solution indicative of emission from the triplet excited state. The photoluminescent spectra for many of these complexes are red-shifted from those observed for the uncoordinated ($HC^{\wedge}N$) ligand precursor. The emission spectra are highly structured with vibrational progressions decreasing in intensity to lower energy. On the basis of the red shift, structured emission pattern, and long luminescent lifetime, i.e., microseconds, the emission is thought to arise from an excited state that is

- (7) (a) Baldo, M. A.; O'Brien, D. F.; You, Y.; Shoustikov, A.; Sibley, S.; Thompson, M. E.; Forrest, S. R. *Nature* **1998**, *395*, 151. (b) Kwong, R. C.; Sibley, S.; Dubovoy, T.; Baldo, M. A.; Forrest, S. R.; Thompson, M. E. *Chem. Mater.* **1999**, *11*, 3709–3713. (c) O'Brien, D. F.; Baldo, M. A.; Thompson, M. E.; Forrest, S. R. *Appl. Phys. Lett.* **1999**, *74*, 442–444. (d) Adachi, C.; Baldo, M. A.; Forrest, S. R.; Lamansky, S.; Thompson, M. E.; Kwong, R. C. *Appl. Phys. Lett.* **2001**, *78*, 1622–1624. (e) Cleave, V.; Yahioglu, G.; Barny, P. L.; Friend, R. H.; Tessler, N. *Adv. Mater.* **1999**, *11*, 285.
- (8) (a) Kunugi, Y.; Mann, K. R.; Miller, L. L.; Exstrom, C. L. *J. Am. Chem. Soc.* **1998**, *120*, 589–590. (b) Chan, S.-C.; Chan, M. C. W.; Wang, Y.; Che, C.-M.; Cheung, K. K.; Zhu, N. *Chem. Eur. J.* **2001**, *7*, 4180–4190. (c) Lu, W.; Mi, B.-X.; Chan, M. C. W.; Hui, Z.; Zhu, N.; Lee, S.-T.; Che, C.-M. *Chem. Commun.* **2002**, 206–207.
- (9) (a) Lamansky, S.; Djurovich, P.; Murphy, D.; Abdel-Razzaq, F.; Lee, H.-E.; Adachi, C.; Burrows, P. E.; Forrest, S. R.; Thompson, M. E. *J. Am. Chem. Soc.* **2001**, *123*, 4304–4312. (b) Lamansky, S.; Djurovich, P.; Murphy, D.; Abdel-Razzaq, F.; Kwong, R.; Tsyba, I.; Bortz, M.; Mui, B.; Bau, R.; Thompson, M. E. *Inorg. Chem.* **2001**, *40*, 1704–1711.
- (10) (a) Baldo, M. A.; Lamansky, S.; Burrows, P. E.; Thompson, M. E.; Forrest, S. R. *Appl. Phys. Lett.* **1999**, *75*, 4–6. (b) Adachi, C.; Baldo, M. A.; Forrest, S. R.; Thompson, M. E. *Appl. Phys. Lett.* **2000**, *77*, 904–906. Ikai, M.; Tokito, S.; Sakamoto, Y.; Suzuki, T.; Taga, Y. *Appl. Phys. Lett.* **2001**, *79*, 156–158.
- (11) Bevilacqua, J. M.; Eisenberg, R. *Inorg. Chem.* **1994**, *33*, 2913–2923.
- (12) Barigelletti, F.; Sandrini, D.; Maestri, M.; Balzani, V.; von Zelewsky, A.; Chassot, L.; Jolliet, P.; Maeder, U. *Inorg. Chem.* **1988**, *27*, 3644–3647.
- (13) Aldridge, T. K.; Stacy, E. M.; McMillin, D. R. *Inorg. Chem.* **1994**, *33*, 722–727.
- (14) (a) Cummings, S. D.; Eisenberg, R. *J. Am. Chem. Soc.* **1996**, *118*, 1949–1960. (b) Zuleta, J. A.; Chesta, C. A.; Eisenberg, R. *J. Am. Chem. Soc.* **1989**, *111*, 8916–8917.

- (15) Whittle, C. E.; Weinstein, J. A.; George, M. W.; Schanze, K. S. *Inorg. Chem.* **2001**, *40*, 4053–4062. Hissler, M.; Connick, W. B.; Geiger, D. K.; McGarrah, J. E.; Lipa, D.; Lachiocotte, R. J.; Eisenberg, R. *Inorg. Chem.* **2000**, *39*, 447. Connick, W. B.; Geiger, D.; Eisenberg, R. *Inorg. Chem.* **1999**, *38*, 3264. Chan, C. W.; Cheng, L. K.; Che, C. M. *Coord. Chem. Rev.* **1994**, *132*, 87.
- (16) Dungey, K. E.; Thompson, B. D.; Kane-Maguire, N. A. P.; Wright, L. L. *Inorg. Chem.* **2000**, *39*, 5192–5196.
- (17) Connick, W. B.; Miskowski, V. M.; Houlding, V. H.; Gray, H. B. *Inorg. Chem.* **2000**, *39*, 2585–2592.
- (18) Lai, S.-W.; Chan, M. C. W.; Cheung, K.-K.; Che, C.-M. *Inorg. Chem.* **1999**, *38*, 4262–4267.
- (19) (a) Cheung, T. C.; Cheung, K. K.; Peng, S. M.; Che, C. M. *J. Chem. Soc., Dalton Trans.* **1996**, 1645–1653. (b) Lai, S.-W.; Chan, C.-W.; Cheung, K.-K.; Che, C.-M. *Organometallics* **1999**, *18*, 3327–3336.
- (20) (a) Chassot, L.; Müller, E.; von Zelewsky, A. *Inorg. Chem.* **1984**, *23*, 4249–4253. (b) Maestri, M.; Sandrini, D.; Balzani, V.; Chasson, L.; Jolliet, P.; von Zelewsky, A. *Chem. Phys. Lett.* **1985**, *122*, 375–379. (c) Chassot, L.; von Zelewsky, A. *Inorg. Chem.* **1987**, *26*, 2814–2818. (d) Jolliet, P.; Gianini, M.; von Zelewsky, A.; Bernardinelli, G.; Stoeckli-Evans, H. *Inorg. Chem.* **1996**, *35*, 4883–4888.
- (21) Deuschel-Cornioley, C.; Lüönd, R.; von Zelewsky, A. *Helv. Chim. Act.* **1989**, *72*, 377–382.
- (22) (a) Kvam, P.-I.; Puzyk, M. V.; Balashev, K. P.; Songstad, J. *Acta Chem. Scand.* **1995**, *49*, 335–343. (b) Mdeleleni, M. M.; Bridgewater, J. S.; Watts, R. J.; Ford, P. C. *Inorg. Chem.* **1995**, *34*, 2334–2342. (c) Balashev, K. P.; Puzyk, M. V.; Kotlyar, V. S.; Kulikova, M. V. *Coord. Chem. Rev.* **1997**, *159*, 109–120. (d) DePriest, J.; Zheng, G. Y.; Goswami, N.; Eichhorn, D. M.; Woods, C.; Rillema, D. P. *Inorg. Chem.* **2000**, *39*, 1955–1963.

predominantly a ^3LC state, mixed with $^1\text{MLCT}$ character by the strong spin-orbit coupling.²³

Heteroleptic $C^{\wedge}N\text{PtLX}$ complexes offer several advantages over the bis- $C^{\wedge}N$ derivatives. Physical properties such as the charge and solubility of the complexes can be independently adjusted through proper choice of the ancillary ligand. It has also been shown that the nature of the ancillary ligand can have profound effects on the lowest emitting excited state.^{22a,c} The electron-donating or -withdrawing character of the LX ligand can increase or decrease the amount of electron density at the metal center. The amount of ground state electron density on the metal will subsequently affect the amount of MLCT character mixed into the lowest energy transition, thus altering both the color of emission and radiative lifetime of the excited state. A series of mixed cyclometalates based on 2-phenylpyridine and 2-thienylpyridine have been reported where LX is an ancillary bidentate ligand based on unsaturated α,α'' -diimines and saturated diamines, such as 2,2'-bipyridine (bpy) or 1,2-diaminoethane (en), respectively.^{22a} It was shown that emission from complexes with unsaturated α,α'' -diimine ligands originates from states on the diimine, rather than those of the cyclometalate. For complexes with saturated LX ligands, the emitting state is strongly governed by the ^3LC transition from the cyclometalate, similar to bis-homoleptic analogues.

We report here a series of cyclometalated platinum complexes of the general structure, $C^{\wedge}N\text{Pt}(O^{\wedge}O)$, where $O^{\wedge}O$ is a β -diketonate ligand, i.e., acetyl acetonate (acac) or dipivalylmethane (dpm). All of these complexes are strongly emissive in frozen glass solutions, and several are strongly emissive in degassed room temperature solution, with lifetimes on the order of microseconds. We observe that the nature of the cyclometalating ligand strongly affects the energy of the emissive state and have been able to tune the emission color throughout the visible spectrum either by modifying the 2-phenylpyridyl ligand with electron-donating and -withdrawing substituents or by varying the character of the cyclometalate. The emission for all of these complexes is attributed to a mixed ^3LC -MLCT state.

Experimental Section

Equipment. The UV-visible spectra were recorded on an Aviv model 14DS spectrophotometer (a re-engineered Cary 14 spectrophotometer). Photoluminescent spectra were measured using a Photon Technology International fluorimeter. Quantum efficiency measurements were carried out at room temperature in a 2-methyltetrahydrofuran solution that was distilled over sodium. Before spectra were measured, the solution was degassed by several freeze-pump-thaw cycles using a diffusion pump. Solutions of coumarin 47 in ethanol ($\Phi = 0.60$) or degassed *fac*-Ir(*ppy*)₃ in 2-MeTHF ($\Phi = 0.40$) were used as a reference. The equation

$$\Phi_s = \Phi_r \left(\frac{\eta_s^2 A_r I_s}{\eta_r^2 A_s I_r} \right)$$

was used to calculate quantum yields where Φ_s is the quantum

yield of the sample, Φ_r is the quantum yield of the reference, η is the refractive index of the solvent, A_s and A_r are the absorbance of the sample and the reference at the wavelength of excitation, and I_s and I_r are the integrated areas of emission bands.^{22d} Steady state emission experiments at room temperature were performed on a PTI QuantaMaster model C-60 spectrofluorimeter. Phosphorescence lifetime measurements were performed on the same fluorimeter equipped with a microsecond Xe flash lamp and were limited to lifetimes $> 2 \mu\text{s}$. NMR spectra were recorded on Bruker AC 250 MHz, AM 360 MHz, or AMX 500 MHz instruments. Solid probe MS spectra were taken with Hewlett-Packard GC/MS instrument with electron impact ionization and model 5873 mass selective detector. The Microanalysis Laboratory at the University of Illinois, Urbana-Champaign, performed all elemental analyses.

Electrochemistry. Cyclic voltammetry and differential pulsed voltammetry were performed using an EG&G potentiostat/galvanostat model 283. Anhydrous DMF (Aldrich) was used as the solvent under a nitrogen atmosphere, and 0.1 M tetra(*n*-butyl)ammonium hexafluorophosphate was used as the supporting electrolyte. A Ag wire was used as the pseudoreference electrode, and a Pt wire was used as the counter electrode. The working electrode was glassy carbon. The redox potentials are based on values measured from differential pulsed voltammetry and are reported relative to a ferrocene/ferrocenium ($\text{Cp}_2\text{Fe}/\text{Cp}_2\text{Fe}^+$) redox couple used as an internal reference (0.45 V vs SCE)²⁴ while electrochemical reversibility was determined using cyclic voltammetry.

X-ray Crystallography. Diffraction data for *thpy*Pt(dpm) was collected at room temperature ($T = 23^\circ\text{C}$) on a Bruker SMART APEX CCD diffractometer with graphite-monochromated Mo K α radiation ($\lambda = 0.71073 \text{ \AA}$). The cell parameters for the Pt complex were obtained from the least-squares refinement of the spots (from 60 collected frames) using the SMART program. A hemisphere of the crystal data was collected up to a resolution of 0.75 \AA , and the intensity data was processed using the Saint Plus program. All calculations for structure determination were carried out using the SHELXTL package (version 5.1).²⁵ Initial atomic positions were located by Patterson methods using XS, and the structure was refined by least-squares methods using SHELX with 6983 independent reflections and within the range of Φ 1.38–24.71° (completeness 98.8%). Absorption corrections were applied by using SADABS.²⁶ Calculated hydrogen positions were input and refined in a riding manner along with the attached carbons. A summary of the refinement details and the resulting factors are given in Table 1.

Density Functional Calculations. DFT calculations were performed using Titan software package (Wavefunction, Inc.) at the B3LYP/LACVP** level. The HOMO and LUMO energies were determined using minimized singlet geometries to approximate the ground state. The minimized singlet geometries were used to calculate the triplet molecular orbitals and approximate the triplet HSOMO (HSOMO = highest singly occupied molecular orbital).

Synthesis of $(C^{\wedge}N)\text{Pt}(O^{\wedge}O)$ Complexes: General Procedure. The compounds 2-bromo-4-methoxypyridine,²⁷ 2-bromo-4-dimethylaminopyridine,²⁸ 2-(1,5-dimethylpyrrol-2-yl)pyridine,²⁹ and

(24) (a) Gagné, R. R.; Koval, C. A.; Lisensky, G. C. *Inorg. Chem.* **1980**, *19*, 2854–2855. (b) Sawyer, D. T.; Sobkowiak, A.; Roberts, J. L., Jr. *Electrochemistry for Chemists*, 2nd ed.; John Wiley and Sons: New York, 1995; pp 467.

(25) Sheldrick, G. M. *SHELXTL*, version 5.1; Bruker Analytical X-ray System, Inc.: Madison, WI, 1997.

(26) Blessing, R. H. *Acta Crystallogr.* **1995**, *A51*, 33–38.

(27) Effenberger, F.; Krebs, A.; Willrett, P. *Chem. Ber.* **1992**, *125*, 1131–1140.

(23) (a) Juris, A.; Balzani, V.; Barigelli, F.; Campagna, S.; Belser, P.; von Zelewsky, A. *Coord. Chem. Rev.* **1988**, *84*, 85–277. (b) Crosby, G. A. *Acc. Chem. Res.* **1975**, *8*, 231–238.

Table 1. Crystal Data and Structure Refinement for *ThpyPt(dpm)*

empirical formula	C ₂₀ H ₂₅ NO ₂ PtS
fw	538.56
temp	296(2) K
wavelength	0.71073 Å
cryst syst	triclinic
space group	<i>P</i> 1
unit cell dimens	
<i>a</i>	10.7376(17) Å
<i>b</i>	13.804(2) Å
<i>c</i>	15.995(3) Å
α	110.487(2)°
β	91.959(3)°
γ	108.925(3)°
vol	2071.5(6) Å ³
<i>Z</i>	4
density (calcd)	1.727 g/cm ³
abs coeff	6.886 mm ⁻¹
<i>F</i> (000)	1048
cryst size	0.35 × 0.13 × 0.05 mm ³
Θ range for data collection	1.38–24.71°
index ranges	–12 ≤ <i>h</i> ≤ 12, –16 ≤ <i>k</i> ≤ 15, –16 ≤ <i>l</i> ≤ 18
reflns collected	10636
indep reflns	6983 [<i>R</i> (int) = 0.0212]
completeness (to $\Theta = 24.71^\circ$)	98.8%
transm factors	min/max ratio 0.663952
refinement meth	full-matrix least squares on <i>F</i> ²
data/restraints/params	6983/0/399
GOF on <i>F</i> ²	0.986
final <i>R</i> indices [<i>I</i> > 2σ(<i>I</i>)]	<i>R</i> 1 = 0.0455, <i>wR</i> 2 = 0.1118
<i>R</i> indices (all data)	<i>R</i> 1 = 0.0637, <i>wR</i> 2 = 0.1215
largest diff peak and hole	1.464 and –0.699 e ⁻ Å ⁻³

2-(2'-benzothienyl)pyridine³⁰ were prepared following literature procedures. 2-Phenylpyridine and *p*-tolylpyridine were purchased from Aldrich Chemical Co. Other phenylpyridine derivatives were prepared by Suzuki coupling reaction with commercially available boronic acids and the appropriate bromopyridines.³¹ All other ligands and materials were purchased from either Aldrich Chemical Co. or Frontier Scientific and used without further purification.

All procedures were carried out in inert gas atmosphere despite the air stability of the complexes, the main concern being the oxidative and thermal stability of intermediates at the high temperatures in the reactions. The Pt(II) μ -dichloro-bridged dimers were prepared by a modified method of Lewis.³² This involves heating the K₂PtCl₄ salt with 2–2.5 equiv of cyclometalating ligand in a 3:1 mixture of 2-ethoxyethanol (Aldrich) and water to 80 °C for 16 h. The dimers were isolated in water and were subsequently reacted with 3 equiv of the chelating diketone derivative and 10 equiv of Na₂CO₃ in 2-ethoxyethanol at 100 °C for 16 h. The solvent was removed under reduced pressure, and the compound was purified by flash chromatography using dichloromethane. The product was recrystallized with dichloromethane/methanol.

Characterization. *ppyPt(acac)*: platinum(II) (2-phenylpyridinato-*N,C*^{2'}) (2,4-pentanedionato-*O,O*). Yield: 36%. ¹H NMR (360 MHz, acetone-*d*₆), ppm: 9.00 (d, 1H, *J* = 5.8 Hz), 8.02 (dd, 1H, *J* = 1.6, 7.4 Hz), 7.89 (d, 1H, *J* = 7.9 Hz), 7.57 (dd, 1H, *J* = 1.6, 7.4 Hz), 7.51 (dd, 1H, *J* = 1.6, 7.4 Hz), 7.32 (dd, 1H, *J* = 1.6, 6.8 Hz), 7.11 (ddd, 1H, *J* = 1.6, 7.9 Hz), 7.04 (dd, 1H, *J* = 1.6, 7.4 Hz), 5.55 (s, 1H), 1.98 (s, 3H), 1.95 (s, 3H). Anal. for C₁₆H₁₅NO₂Pt: found C 43.13, H 3.41, N 3.42, calcd C 42.86, 3.37, 3.12.

(28) Sammakia, T.; Hurley, T. B. *J. Org. Chem.* **1999**, *64*, 4652–4664.

(29) Savoia, D.; Concialini, V.; Tarsi, L. *J. Org. Chem.* **1991**, *56*, 1822–1827.

(30) (a) Chippendale, K. E.; Iddon, B.; Suschitzky, H. *J. Chem. Soc., Perkin Trans.* **1972**, 2023–2030. (b) Gilman, H.; Shirley, D. A. *J. Am. Chem. Soc.* **1949**, *90*, 1871.

(31) Lohse, O.; Thevenin, P.; Waldvogel, E. *Synlett* **1999**, *1*, 45–48.

ppyPt(dpm): platinum(II) (2-phenylpyridinato-*N,C*^{2'}) (2,2,6,6-tetramethyl-3,5-heptanedionato-*O,O*). Yield: 30%. ¹H NMR (250 MHz, CDCl₃), ppm: 8.98 (d, 1H, *J* = 6.2 Hz), 7.77 (dd, 1H, *J* = 8.4, 9.5, 1.8 Hz), 7.62 (m, 2H), 7.42 (dd, 1H, *J* = 7.7, 1.1 Hz), 7.19 (ddd, 1H, *J* = 7.7, 8.8, 1.5 Hz), 7.08 (m, 2H), 5.79 (s, 1H), 1.26 (s, 9H), 1.25 (s, 9H). Anal. for C₂₂H₂₇NO₂Pt: found C 49.94, H 5.11, N 2.69, calcd C 49.62, H 5.11, N 2.63.

tpyPt(acac): platinum(II) (2-(*p*-tolyl)pyridinato-*N,C*^{2'}) (2,4-pentanedionato-*O,O*). Yield: 42%. ¹H NMR (360 MHz, CDCl₃), ppm: 8.94 (d, 1H, *J* = 5.9 Hz), 7.74 (d, 1H, *J* = 6.8 Hz), 7.53 (d, 1H, *J* = 7.8 Hz), 7.39 (s, 1H), 7.30 (d, 1H, *J* = 7.8 Hz), 7.04 (d, 1H, *J* = 6.8 Hz), 6.88 (d, 1H, *J* = 7.8 Hz), 5.45 (s, 1H), 2.00 (s, 3H), 1.98 (s, 3H), 1.95 (s, 3H). Anal. for C₁₇H₁₇NO₂Pt: found C 44.10, H 3.89, N 3.32, calcd C 44.16; H 3.71; N 3.03.

tpyPt(dpm): platinum(II) (2-(*p*-tolyl)pyridinato-*N,C*^{2'}) (2,2,6,6-tetramethyl-3,5-heptanedionato-*O,O*). Yield: 40%. ¹H NMR (250 MHz, CDCl₃), ppm: 8.94 (d, 1H, *J* = 5.9 Hz), 7.74 (dd, 1H, *J* = 9.1, 8.4, 1.5 Hz), 7.54 (d, 1H, *J* = 8.04 Hz), 7.45 (s, 1H), 7.31 (d, 1H, *J* = 7.7 Hz), 7.04 (dd, 1H, *J* = 5.9, 8.4, 1.1 Hz), 6.89 (d, 1H, *J* = 7.7 Hz), 5.78 (s, 1H), 2.38 (s, 3H), 1.27 (s, 9H), 1.25 (s, 9H). Anal. for C₂₃H₂₉NO₂Pt: found C 49.18, H 5.13, N 2.64, calcd C 50.54, H 5.35, N 2.56.

otpyPt(acac): platinum(II) (2-(*o*-tolyl)pyridinato-*N,C*^{2'}) (2,4-pentanedionato-*O,O*). Yield: 29%. ¹H NMR (250 MHz, CDCl₃), ppm: 9.41 (d, 1H, *J* = 5.9 Hz), 7.81 (m, 2H), 7.56 (d, 1H, *J* = 7.7 Hz), 7.06 (m, 2H), 6.87 (d, 1H, *J* = 7.3 Hz), 5.44 (s, 1H), 2.64 (s, 3H), 1.98 (s, 3H), 1.97 (s, 3H). Anal. for C₁₇H₁₇NO₂Pt: found C 44.05, H 3.55, N 3.06, calcd C 44.16, H 3.71, N 3.03.

6FppyPt(dpm): platinum(II) (2-(6'-fluorophenyl)pyridinato-*N,C*^{2'}) (2,2,6,6-tetramethyl-3,5-heptanedionato-*O,O*). Yield: 25%. ¹H NMR (250 MHz, CDCl₃), ppm: 9.04 d, 1H, *J* = 5.8 Hz), 8.03 (d, 1H, *J* = 8.2 Hz), 7.81 (dd, 1H, *J* = 8.2, 8.2 Hz), 7.45 (d, 1H, *J* = 7.2 Hz), 7.15 (m, 2H), 6.77 (ddd, 1H, *J* = 12.3, 8.2, 1.0 Hz), 5.80 (s, 1H), 1.26 (s, 9H), 1.25 (s, 9H). Anal. for C₂₂H₂₆FNO₂Pt: found C 48.07, H 4.83, N 2.68, calcd C 48.00, H 4.76, N 2.54.

6tfmppyPt(dpm): platinum(II) (2-(6'-trifluoromethylphenyl)pyridinato-*N,C*^{2'}) (2,2,6,6-tetramethyl-3,5-heptanedionato-*O,O*). Yield: 30%. ¹H NMR (250 MHz, CDCl₃), ppm: 9.20 (d, 1H, *J* = 6.1 Hz), 8.08 (d, 1H, *J* = 8.5 Hz), 7.99 (d, 1H, *J* = 7.5 Hz), 7.84 (ddd, 1H, *J* = 8.8, 7.5, 1.7 Hz), 7.47 (d, 1H, *J* = 7.8 Hz), 7.12 (m, 2H), 5.81 (s, 1H), 1.27 (s, 9H), 1.26 (s, 9H). Anal. for C₂₃H₂₆F₃NO₂Pt: found C 45.86, H 4.32, N 2.38, calcd C 46.00, H 4.36, N 2.33.

45dfppyPt(acac): platinum(II) (2-(4',5'-difluorophenyl)pyridinato-*N,C*^{2'}) (2,4-pentanedionato-*O,O*). Yield: 37%. ¹H NMR (360 MHz, acetone-*d*₆), ppm: 8.99 (d, 1H, *J* = 5.7 Hz), 8.06 (dd, 1H, *J* = 2.3, 8.0 Hz), 7.90 (d, 1H, *J* = 8.0 Hz), 7.62–7.68 (m, 1H), 7.37 (ddd, 1H, *J* = 1.7, 5.7 Hz), 7.20–7.25 (m, 1H), 5.58 (s, 1H), 1.99 (s, 3H), 1.98 (s, 3H). Anal. for C₁₆H₁₃F₂NO₂Pt: found C 39.40, 2.91, 2.61, calcd C 39.68, H 2.71, N 2.89.

46dfppyPt(acac): platinum(II) (2-(4',6'-difluorophenyl)pyridinato-*N,C*^{2'}) (2,4-pentanedionato-*O,O*). Yield: 47%. ¹H NMR (250 MHz, CDCl₃), ppm: 8.95(d, 1H, *J* = 5.8 Hz), 7.91 (d, 1H, *J* = 8.2 Hz), 7.79 (m, 2H), 7.08 (m, 2H), 6.54 (ddd, 1H, *J* = 11.6, 9.3, 2.4 Hz), 5.45 (s, 1H), 1.99 (s, 3H), 1.98 (s, 3H). Anal. for C₁₆H₁₃F₂NO₂Pt: found C 39.52, H 2.56, N 2.87, calcd C 39.68, H 2.71, N 2.89.

46dfppyPt(dpm): platinum(II) (2-(4',6'-difluorophenyl)pyridinato-*N,C*^{2'}) (2,2,6,6-tetramethyl-3,5-heptanedionato-*O,O*). Yield: 38%. ¹H NMR (250 MHz, CDCl₃), ppm: 9.00 (d, 1H, *J* = 6.1

(32) Cockburn, B. N.; Howe, D. V.; Keating, T.; Johnson, B. F. G.; Lewis, J. J. *J. Chem. Soc., Dalton Trans.* **1973**, 404–410.

Hz), 7.96 (d, 1H, $J = 8.5$ Hz), 7.81 (dd, 1H, $J = 7.5, 7.5$ Hz), 7.11 (m, 2H), 6.55 (ddd, 1H, $J = 11.7, 9.4, 2.4$ Hz), 5.81 (s, 1H), 1.26 (s, 9H), 1.25 (s, 9H). Anal. for $C_{22}H_{25}F_2NO_2Pt$: found C 46.33, H 4.35, N 2.55, calcd C 46.48, H 4.43, N 2.46.

46dfp-3MepyPt(dpm): platinum(II) (2-(4',6'-difluorophenyl)-3-methylpyridinato- N, C^2) (2,2,6,6-tetramethyl-3,5-heptanedionato- O, O). Yield: 25%. 1H NMR (250 MHz, $CDCl_3$), ppm: 8.98 (d, 1H, $J = 5.8$ Hz), 7.65 (d, 1H, $J = 7.9$ Hz), 7.17 (dd, 1H, $J = 8.5, 2.7$ Hz), 7.07 (dd, 1H, $J = 7.8, 5.8$ Hz), 6.53 (m, 1H), 5.80 (s, 1H), 2.53 (d, 3H, $J = 11.6$ Hz), 1.25 (s, 9H), 1.24 (s, 9H). Anal. for $C_{23}H_{27}F_2NO_2Pt$: found C 47.24, H 4.57, N 2.51, calcd C 47.42, H 4.67, N 2.46.

46dfp-4MepyPt(dpm): platinum(II) (2-(4',6'-difluorophenyl)-4-methylpyridinato- N, C^2) (2,2,6,6-tetramethyl-3,5-heptanedionato- O, O). Yield: 30%. 1H NMR (250 MHz, $CDCl_3$), ppm: 8.80 (d, 1H, $J = 5.4$ Hz), 7.77 (s, 1H), 7.10 (dd, 1H, $J = 8.2, 2.4$ Hz), 6.96 (d, 1H, $J = 6.8$ Hz), 6.55 (ddd, 1H, $J = 12.2, 9.2, 2.4$ Hz), 5.80 (s, 1H), 2.43 (s, 3H), 1.25 (s, 9H), 1.24 (s, 9H). Anal. for $C_{23}H_{27}F_2NO_2Pt$: found C 47.22, H 4.05, N 2.41, calcd C 47.42, H 4.67, N 2.40.

46dfp-5MepyPt(dpm): platinum(II) (2-(4',6'-difluorophenyl)-5-methylpyridinato- N, C^2) (2,2,6,6-tetramethyl-3,5-heptanedionato- O, O). Yield: 31%. 1H NMR (250 MHz, $CDCl_3$), ppm: 8.84 (s, 1H), 7.83 (d, 1H, $J = 8.5$ Hz), 7.62 (d, 1H, $J = 8.5$ Hz), 7.09 (dd, 1H, $J = 8.8, 2.7$ Hz), 6.54 (ddd, 1H, $J = 11.9, 9.5, 2.7$ Hz), 5.81 (s, 1H), 2.38 (s, 3H), 1.26 (s, 9H), 1.25 (s, 9H). Anal. for $C_{23}H_{27}F_2NO_2Pt$: found C 47.40, H 4.64, N 2.49, calcd C 47.42, H 4.67, N 2.40.

46dfp-6MepyPt(dpm): platinum(II) (2-(4',6'-difluorophenyl)-6-methylpyridinato- N, C^2) (2,2,6,6-tetramethyl-3,5-heptanedionato- O, O). Yield: 5%. 1H NMR (250 MHz, $CDCl_3$), ppm: 7.86 (d, 1H, $J = 7.2$ Hz), 7.64 (dd, 1H, $J = 8.2, 8.2$ Hz), 7.20 (dd, 1H, $J = 9.6, 2.7$ Hz), 6.96 (d, 1H, $J = 8.2$ Hz), 6.55 (ddd, 1H, $J = 11.9, 8.9, 2.4$ Hz), 5.85 (s, 1H), 3.04 (s, 3H), 1.26 (s, 9H), 1.19 (s, 9H). Anal. for $C_{23}H_{27}F_2NO_2Pt$: found C 47.01, H 4.26, N 2.44, calcd C 47.42, H 4.67, N 2.40.

46dFp-4meopyPt(acac): platinum(II) (2-(4',6'-difluorophenyl)-4-methoxyppyridinato- N, C^2) (2,4-pentanedionato- O, O). Yield: 21%. 1H NMR (250 MHz, $CDCl_3$), ppm: 8.70 (d, 1H, $J = 7.0$ Hz), 7.45 (dd, 1H, $J = 2.9$ Hz), 7.06 (dd, 1H, $J = 8.8, 2.6$ Hz), 6.68 (dd, 1H, $J = 6.6, 2.9$ Hz), 6.53 (ddd, 1H, $J = 11.7, 9.1, 2.6$ Hz), 5.45 (s, 1H), 1.98 (s, 3H), 1.97 (s, 3H). Anal. for $C_{17}H_{15}F_2NO_3Pt$: found C 39.16, H 2.39, N 2.61, calcd C 39.69, H 2.94, N 2.72.

46dFp-4meopyPt(dpm): platinum(II) (2-(4',6'-difluorophenyl)-4-methoxyppyridinato- N, C^2) (2,2,6,6-tetramethyl-3,5-heptanedionato- O, O). Yield: 22%. 1H NMR (250 MHz, $CDCl_3$), ppm: 8.71 (d, 1H, $J = 6.8$ Hz), 7.47 (dd, 1H, $J = 2.7, 2.7$ Hz), 7.07 (dd, 1H, $J = 8.2, 2.1$ Hz), 6.69 (dd, 1H, $J = 6.8, 2.7$ Hz), 6.54 (ddd, 1H, $J = 11.9, 9.2, 2.4$ Hz), 5.46 (s, 1H), 3.93 (s, 3H), 1.98 (s, 3H), 1.97 (s, 3H). Anal. for $C_{23}H_{27}F_2NO_3Pt$: found C 45.94, H 4.36, N 2.45, calcd C 46.15, H 4.55, N 2.34.

46dFp-4dmapyPt(dpm): platinum(II) (2-(4',6'-difluorophenyl)-4-dimethylaminopyridinato- N, C^2) (2,2,6,6-tetramethyl-3,5-heptanedionato- O, O). Yield: 20%. 1H NMR (250 MHz, $CDCl_3$), ppm: 8.42 (d, 1H, $J = 6.6$ Hz), 7.17 (dd, 1H, $J = 2.94, 2.94$ Hz), 7.08 (dd, 1H, $J = 8.8, 2.9$ Hz), 6.51 (ddd, 1H, $J = 11.7, 8.83, 2.9$ Hz), 6.36 (dd, 1H, $J = 6.6, 2.9$ Hz), 5.76 (s, 1H), 3.10 (s, 6H), 1.24 (s, 9H), 1.23 (s, 9H). Anal. for $C_{24}H_{30}F_2N_2O_2Pt$: found C 46.97, H 4.78, N 4.57, calcd C 47.13, H 4.94, N 4.58.

4meopyPt(dpm): platinum(II) (2-(4'-methoxyphenyl)pyridinato- N, C^2) (2,2,6,6-tetramethyl-3,5-heptanedionato- O, O). Yield: 28%. 1H NMR (250 MHz, $CDCl_3$), ppm: 8.88 (d, 1H, $J = 4.9$ Hz), 7.71 (d, 1H, $J = 9.2, 9.2, 1.8$ Hz), 7.45 (d, 1H, $J = 7.9$ Hz), 7.35 (d,

1H, $J = 8.5$ Hz), 7.20 (d, 1H, $J = 2.4$ Hz), 6.98 (m, 1H), 6.65 (dd, 1H, $J = 8.5, 3.1$ Hz), 5.79 (s, 1H), 3.86 (s, 3H), 1.26 (s, 9H), 1.25 (s, 9H). Anal. for $C_{23}H_{29}NO_3Pt$: found C 47.24, H 4.57, N 2.51, calcd C 47.42, H 4.67, N 2.46.

5meopyPt(dpm): platinum(II) (2-(5'-methoxyphenyl)pyridinato- N, C^2) (2,2,6,6-tetramethyl-3,5-heptanedionato- O, O). Yield: 25%. 1H NMR (250 MHz, $CDCl_3$), ppm: 8.97 (d, 1H, $J = 5.5$ Hz), 7.78 (ddd, 1H, $J = 8.1, 9.1, 1.8$ Hz), 7.57 (s, 1H), 7.51 (d, 1H, $J = 8.4$ Hz), 7.09 (ddd, 1H, $J = 8.8, 5.9, 1.1$ Hz), 7.01 (d, 1H, $J = 2.6$ Hz), 6.90 (dd, 1H, $J = 8.4, 2.6$ Hz), 5.77 (s, 1H), 1.25 (s, 9H), 1.24 (s, 9H). Anal. for $C_{23}H_{29}NO_3Pt$: found C 48.90, H 4.94, N 2.62, calcd C 49.11, H 5.20, N 2.49.

pqPt(dpm): platinum (II) (2-phenylquinolyl- N, C^2) (2,2,6,6-tetramethyl-3,5-heptanedionato- O, O). Yield: 19%. 1H NMR (250 MHz, $CDCl_3$), ppm: 9.65 (d, 1H, $J = 8.8$ Hz), 8.23 (d, 1H, $J = 8.3$ Hz), 7.77 (m, 4H), 7.54 (m, 2H), 7.17 (m, 2H), 5.89 (s, 1H), 1.30 (s, 9H), 1.27 (s, 9H). Anal. for $C_{20}H_{27}NO_2Pt$: found C 52.95, H 4.74, N 2.53, calcd C 53.60, H 5.02, N 2.40.

btPt(dpm): platinum(II) bis(2-phenylbenzothiazolato- N, C^2) (2,2,6,6-tetramethyl-3,5-heptanedionato- O, O). Yield: 23%. 1H NMR (250 MHz, $CDCl_3$), ppm: 9.34 (d, 1H, $J = 8.2$), 7.78 (m, 2H), 7.52 (m, 2H), 7.41 (m, 1H), 7.20 (m, 1H), 7.09 (m, 1H), 5.89 (s, 1H), 1.33 (s, 9H), 1.29 (s, 9H). Anal. for $C_{26}H_{29}NO_2Pt$: found C 48.05, H 4.16, N 2.41, calcd C 48.97, H 4.62, N 2.38.

btPt(acac): platinum(II) (2-(2'-(4',5'-benzo)thienyl)pyridinato- N, C^3) (2,4-pentanedionato- O, O). Yield: 20%. 1H NMR (360 MHz, $CDCl_3$), ppm: 8.90 (d, 1H, $J = 5.9$ Hz), 8.75–9.79 (m, 1H), 7.77–7.81 (m, 1H), 7.71 (dd, 1H, $J = 1.5, 7.8$ Hz), 7.27–7.34 (m, 3H), 6.95 (dd, 1H, $J = 1.5, 6.8$ Hz), 5.54 (s, 1H), 2.08 (s, 3H), 2.01 (s, 3H). Anal. for $C_{18}H_{15}NO_2PtS$: found C 42.51, H 3.53, N 2.56, calcd C 42.86, 3.00, 2.78.

c6Pt(acac): platinum(II) (3-(2-benzothiazolyl)-7-(diethylamino)-2H-1-benzopyran-2-onato- N', C^4) (2,4-pentanedionato- O, O). Yield: 10%. 1H NMR (250 MHz, $CDCl_3$), ppm: 8.93 (d, 1H, $J = 8.8$ Hz), 7.73 (d, 1H, $J = 7.5$ Hz), 7.33 (m, 2H), 6.49 (d, 1H, $J = 9.5$ Hz), 6.35 (s, 1H), 5.50 (s, 1H), 3.43 (q, 4H, $J = 7.16$ Hz), 1.99 (s, 3H), 1.91 (s, 3H), 1.23 (t, 6H, $J = 7.2$ Hz). Anal. for $C_{25}H_{24}N_2O_4PtS$: found C 46.36, H 3.53, N 4.17, calcd C 46.65, H 3.76, N 4.35.

dpoPt(dpm): platinum(II) (2,4-diphenyloxazolato-1,3- N, C^2) (2,2,6,6-tetramethyl-3,5-heptanedionato- O, O). Yield: 6%. 1H NMR (250 MHz, $CDCl_3$), ppm: 7.71 (d, 2H, $J = 8.5$ Hz), 7.66 (d, 1H, $J = 7.9$ Hz), 7.45 (m, 5H), 7.20 (dd, 1H, $J = 7.5, 1.4$ Hz), 7.08 (ddd, 1H, $J = 8.5, 7.5, 1.0$ Hz), 5.81 (s, 1H), 1.27 (s, 9H), 1.26 (s, 9H). Anal. for $C_{26}H_{29}NO_3Pt$: found C 51.03, H 5.13, N 2.21, calcd C 52.17, H 4.88, N 2.34.

thpyPt(acac): platinum(II) (2-(2'-thienyl)pyridinato- N, C^3) (2,4-pentanedionato- O, O). Yield: 20%. 1H NMR (500 MHz, $CDCl_3$), ppm: 8.78 (d, 1H), 7.67 (m, 1H), 7.46 (d, 1H), 7.26 (d, 1H), 7.17 (d, 1H), 6.86 (m, 1H), 5.46 (s, 1H), 1.98 (s, 3H), 1.95 (s, 3H). Anal. for $C_{14}H_{13}NO_2PtS$: found C 38.10, H 3.02, N 3.21, calcd C 37.00, H 2.88, N 3.08.

thpyPt(dpm): platinum(II) (2-(2'-thienyl)pyridinato- N, C^3) (2,2,6,6-tetramethyl-3,5-heptanedionato- O, O). Yield: 22%. 1H NMR (250 MHz, $CDCl_3$), ppm: 8.79 (d, 1H, $J = 5.8$ Hz), 7.65 (ddd, 1H, $J = 9.2, 7.5, 1.7$ Hz), 7.47 (d, 1H, $J = 4.8$ Hz), 7.27 (d, 1H, $J = 8.5$ Hz), 7.18 (d, 1H, $J = 4.8$ Hz), 6.90 (ddd, 1H, $J = 7.2, 5.8, 1.4$ Hz), 5.79 (s, 1H), 1.25 (s, 9H), 1.23 (s, 9H). Anal. for $C_{20}H_{25}NO_2PtS$: found C 44.57, H 4.70, N 2.74, calcd C 44.60, H 4.68, N 2.60.

pyrpyPt(acac): platinum(II) (2-(1',5'-dimethyl-pyrrol-2'-yl)pyridinato- N, C^2) (2,4-pentanedionato- O, O). Yield: 16%. 1H NMR (250 MHz, $CDCl_3$), ppm: 8.70 (d, 1H, $J = 6.3$ Hz), 7.44 (m, 1H),

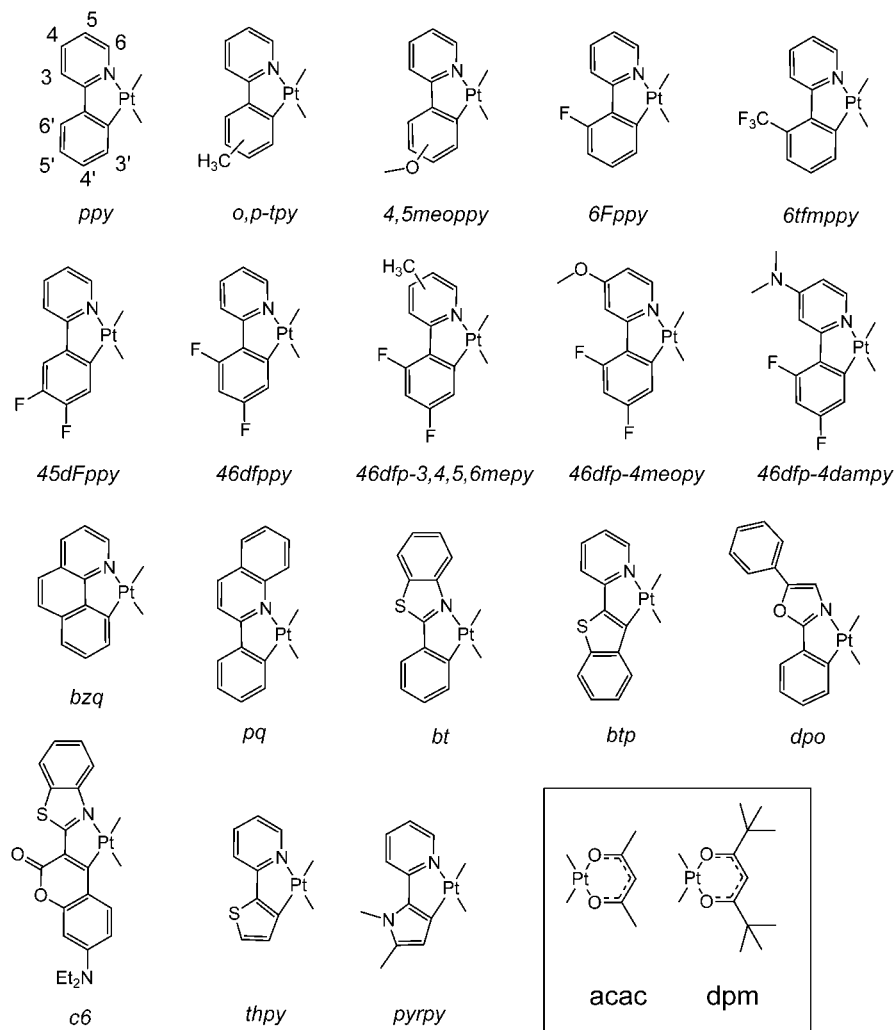


Figure 1. Cyclometalating ligands used to prepare $C^N Pt(O^O)$ complexes. Abbreviations used throughout the paper are listed below the C^N or O^O fragment.

7.05 (d, 1H, $J = 8.5$ Hz), 6.58 (m, 1H), 5.92 (s, 1H), 5.40 (s, 1H), 3.71 (s, 3H), 2.23 (s, 3H), 1.92 (s, 3H), 1.89 (s, 3H). Anal. for $C_{16}H_{18}N_2O_2Pt$: found C 41.48, H 3.90, N 5.53, calcd C 41.29, H 3.90, N 6.02.

ppyPt(dpm): platinum(II) (2-(1',5'-dimethyl-pyrrol-2'-yl)pyridinato- N,C^2) (2,2,6,6-tetramethyl-3,5-heptanedionato- O,O). Yield: 20%. 1H NMR (250 MHz, $CDCl_3$), ppm: 8.70 (d, 1H, $J = 6.1$ Hz), 7.45 (ddd, 1H, $J = 8.8, 7.5, 1.7$ Hz), 7.06 (d, 1H, $J = 8.2$ Hz), 6.59 (ddd, 1H, $J = 7.2, 5.8, 1.4$ Hz), 5.90 (s, 1H), 5.72 (s, 1H), 3.71 (s, 3H), 2.23 (s, 3H), 1.22 (s, 9H), 1.20 (s, 9H). Anal. for $C_{22}H_{30}N_2O_2Pt$: found C 48.39, H 5.60, N 4.91, calcd C 48.08, H 5.50, N 5.10.

bzqPt(acac): platinum(II) (7,8-benzoquinolinato- N,C^3) (2,4-pentanedionato- O,O). Yield: 27%. 1H NMR (360 MHz, acetone- d_6), ppm: 9.13 (d, 1H, $J = 5.4$ Hz), 8.25 (d, 1H, $J = 8.3$ Hz), 7.75 (m, 2H), 7.50–7.57 (m, 3H), 7.44 (dd, 1H, $J = 5.4, 5.4$ Hz), 5.52 (s, 1H), 2.04 (s, 6H). Anal. for $C_{18}H_{15}NO_2Pt$: found C 45.60, H 3.11, N 2.93, calcd C 45.77; H 3.20; N 2.97.

bzqPt(dpm): platinum(II) (7,8-benzoquinolinato- N,C^3) (2,2,6,6-tetramethyl-3,5-heptanedionato- O,O). Yield: 31%. 1H NMR (250 MHz, $CDCl_3$), ppm: 9.12 (d, 1H, $J = 5.5$ Hz), 8.25 (dd, 1H, $J = 8.0, 1.5$ Hz), 7.77 (m, 2H), 7.51 (m, 5H), 5.85 (s, 1H), 1.31 (s, 9H), 1.30 (s, 9H). Anal. for $C_{24}H_{27}NO_2Pt$: found C 51.19, H 4.76, N 2.59, calcd C 51.79, H 4.89, N 2.52.

Results and Discussion

Synthesis and Structure. Dichloride-bridged dimers of the general structure $C^N Pt(\mu-Cl)_2 Pt C^N$ were prepared by the reaction of potassium tetrachloroplatinate with a cyclometalating ligand precursor (HC^N) in 2-ethoxyethanol (eq 1). The structures of the C^N ligands used are shown in



Figure 1. The dimers were isolated as solids that varied in color from gray to red, depending on the purity of the dimer complex and identity of the chelating ligand. Related square planar dimers have been well characterized in the literature.^{22b,33} In most instances, the dimers were not further characterized and were used directly in subsequent reactions. The dimers were dissociated in the presence of a base and either acetyl

(33) (a) Balashev, K. P.; Simon, J.; Ford, P. C. *Inorg. Chem.* **1991**, *30*, 859–861. (b) Pregosin, P. S.; Wombacher, F.; Albinati, A.; Lianza, F. *J. Organomet. Chem.* **1991**, *418*, 249–267. (c) Cope, A. C.; Siekman, R. W. *J. Am. Chem. Soc.* **1965**, *87*, 3272–3273. (d) Cave G. W. V.; Fanizzi F. P.; Deeth R. J.; Errington, W.; Rourke, J. P. *Organometallics* **2000**, *19*, 1355–1364. (e) Nonoyama, M.; Takayanagi, H. *Transition Met. Chem.* **1976**, *1*, 10–13.

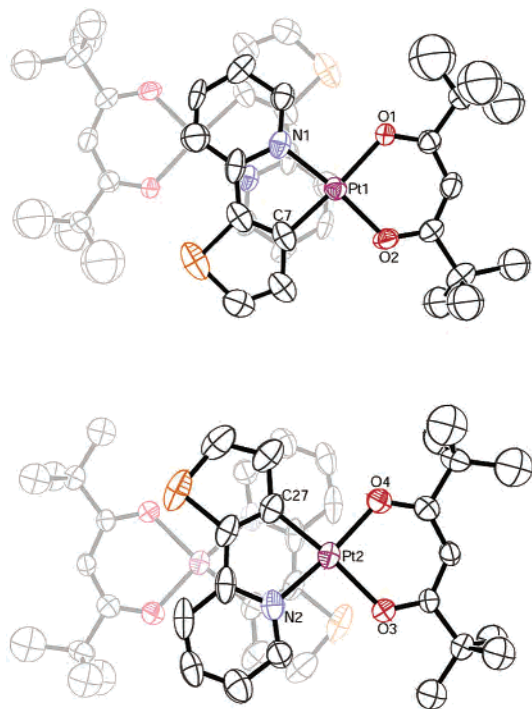
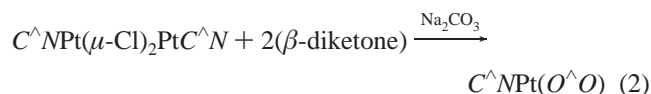


Figure 2. ORTEP diagram of two *thpyPt(dpm)* dimers. One of the *thpyPt(dpm)* molecules in each dimer has been lightened in color for clarity.

acetone (*acacH*) or dipivaloylmethane (*dpmH*) (eq 2). The



isolated yields for these complexes, based on K_2PtCl_4 , varied between 5% and 50%. The complexes have the general structure $C^{\wedge}NPt(O^{\wedge}O)$, as shown in Figure 1, are air stable and sublimable, and varied in color between yellow and red. Changing the ancillary β -diketonate ligand from *acac* to *dpm* increases the solubility of the complexes and greatly simplifies purification by column chromatography. The increased solubility also allows for photophysical measurements to be made in solvents having a broad range of polarities, such as THF or hexanes. Our synthesis is quite general, and complexes can be easily prepared with a variety of functional groups on the $C^{\wedge}N$ ligand. The synthesis of the bis-cyclometalated analogues, in contrast, requires use of more reactive organolithium intermediates that are intolerant of many of the functional groups used here.^{20a,c} In addition, our synthesis avoids the use of thallium acetyl acetonate, which has been previously employed to prepare Pt(II) *acac* complexes.^{32,34}

Crystal Structure. Single crystals of *thpyPt(dpm)* were grown from dichloromethane/methanol solution and characterized using X-ray crystallography. There are two unique molecules in the asymmetric unit. The molecules pack as head-to-tail dimers, each molecule of the dimer related to the other by a center of inversion (Figure 2). The dimers have a plane-to-plane separation of 3.45 Å for Pt(1) and 3.56

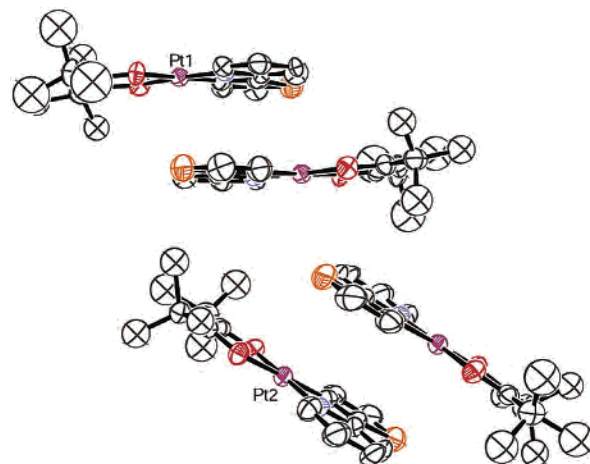


Figure 3. ORTEP diagram showing π stacking of *thpyPt(dpm)*.

Å for Pt(2) indicative of moderate π - π interactions (Figure 3). There are no metal-metal interactions, the closest Pt-Pt distance being 4.92 Å. Each molecule has a distorted square planar geometry. The Pt(1)-C(7) (1.953(7) Å), Pt(2)-C(27) (1.983(7) Å) bond lengths are similar to the mean value reported for the *cis*-(*thpy*)₂Pt complex (1.989(6) Å).³⁵ The Pt(1)-N(1) (1.984(5) Å), Pt(2)-N(2) (2.006(6) Å) bond lengths are slightly larger and comparable to mean values of 2.05 Å from other (*thpy*)Pt derivatives where N is opposite a ligand of weak trans influence.³⁶ The Pt(1)-O(1) (2.064(4) Å), Pt(1)-O(2) (1.998(4) Å) and Pt(2)-O(3) (2.083(4) Å), Pt(2)-O(4) (1.990(4) Å) bond lengths are within the 1.985(6)-2.156(15) Å range of other cyclometalated Pt(β -diketonato) derivatives³⁴ with the longer distances corresponding to oxygen trans to carbon. The C(7)-Pt(1)-N(1) (81.7(3)°), C(27)-Pt(2)-N(2) (80.9(3)°) and O(1)-Pt(1)-O(2) (92.26(16)°), O(3)-Pt(2)-O(4) (92.28(17)°) bond angles are typical for cyclometalates and β -diketonate derivatives of Pt.^{34,37} There is very little distortion away from the square plane, and the C-Pt-N and O-Pt-O chelate planes are only slight bowed and subtend angles of 4.57° for Pt(1) and 3.36° for Pt(2).

DFT Calculations. B3LYP density functional theory (DFT) calculations were carried out on several of the $C^{\wedge}NPt$ -(*acac*) complexes using a LACVP** basis set. A similar approach has been used to investigate the ground and excited state properties of related Ir complexes (i.e., Ir(*ppy*)₃ and (*ppy*)₂Ir(*acac*)).³⁸ We will focus our discussion here on the results for *ppyPt(acac)*; however, all of the $C^{\wedge}NPt$ -(*acac*) complexes we examined gave a similar picture of the HOMO and LUMO orbitals. The calculated values for Pt-C (1.98 Å), Pt-N (2.03 Å), Pt-O (2.04 Å), and Pt-O (2.15 Å) bond lengths and C-Pt-N (81.2°) and O-Pt-O (90.9°) chelate angles compare favorably to the corresponding experimental values determined in the X-ray structure of *thpyPt(dpm)* and

(34) Ghedini, M.; Pucci, D.; Crispini, A.; Barberio, G. *Organometallics* **1999**, *18*, 2116-2124.

(35) Breu, J.; Range, K.-J.; von Zelewsky, A.; Yersin, H. *Acta Crystallogr.* **1997**, *C53*, 562-565.

(36) (a) Stückli, A. C.; Klement, U.; Range, K.-J. *Z. Kristallogr.* **1993**, *208*, 297-298. (b) Giordano, T. J.; Rasmussen, P. G. *Inorg. Chem.* **1975**, *14*, 1628-1634.

(37) Katoh, H.; Miki, K.; Kai, Y.; Tanaka, N.; Kasai, N. *Bull. Chem. Soc. Jpn.* **1981**, *54*, 611-612.

(38) Hay, P. J. *J. Phys. Chem. A* **2002**, *106*, 1634.

Table 2. Absorption, 77 K Emission, and Redox Properties of $C^{\wedge}N$ Pt($O^{\wedge}O$) Complexes

$C^{\wedge}N$	LX	abs, λ_{\max}^a λ (nm) $\{\epsilon$ (10^{-3} cm $^{-1}$ M $^{-1}$) $\}$	emission at 77 K b		redox (V) c $E_{1/2}^{\text{Red}}$
			λ_{\max} (nm)	τ (μ s)	
<i>ppy</i>	dpm	249 (28), 286 (19), 322 (8.8), 333(8.9), 381 (6.6), 406 (2.8), 430 sh (1.8)	477	8.9	-2.41
<i>ppy</i>	acac	269 (32), 292 (28), 310 (22), 360 (11), 389 (6.0), 410 sh (3.7)	480	9.0	-2.39
<i>p-tpy</i>	acac	252 (28), 281 (22), 317 (11), 330 (9.7), 360 (6.6), 398 sh (3.1)	480	10.9	-2.34
<i>o-tpy</i>	acac	254 (31), 281 (19), 316 (11), 328 (11), 368 (5.7), 404 sh (2.7)	480	8.6	-2.39
<i>6fppy</i>	dpm	246 (33), 284 (18), 317 (10), 329 (12), 363 (4.7), 381 (6.9), 410 (2.9)	468	7.2	-2.37
<i>6fmpy</i>	dpm	240 (24), 257 (27), 281 (22), 305 (11), 326 sh (9.4), 395 (7.0), 420 sh (3.7)	487	7.7	-2.14
<i>46dfppy</i>	dpm	280 (20), 315 (11), 327 (12), 358 (5.7), 373 (8.0), 394 (3.1)	458	8.1	-2.31
<i>46dfppy</i>	acac	252 (30), 273 sh (19), 308 (11), 321 (11), 359 (6.9), 390 sh (2.4)	458	9.1	-2.29
<i>45dfppy</i>	acac	274 (22), 312 (10), 323 (8.9), 361 (6.0) 400 sh (2.3)	476	10.5	-2.27
<i>46dfp-3mepy</i>	dpm	247 (28), 280 (17), 317 (11), 330 (10), 377 (6.0), 400 (2.9)	467	9.1	-2.38
<i>46dfp-4mepy</i>	dpm	246 (34), 279 (20), 312 (11), 324 (11), 369 (8.1), 390 (3.2)	456	7.7	-2.42
<i>46dfp-5mepy</i>	dpm	246 (28), 281 (16), 315 (9.0), 329 (10), 369 (6.1), 395 (2.1)	466	10.0	-2.32
<i>46dfp-6mepy</i>	dpm	246 (21), 276 (16), 315 (8.1), 330 (9.7), 373 (5.4), 396 (2.8)	464	11.5	-2.31
<i>46dfp-4meopy</i>	dpm	211 (23), 246 (30), 276 (20), 306 (9.0), 349 (6.1), 367 (7.7)	438	7.0	-2.51
<i>46dfp-4dmapy</i>	dpm	214 (9.2), 244 (15), 277 (16), 348 (4.5), 365 (6.0)	440	6.1	-2.60
<i>4meopy</i>	dpm	249 (25), 270 (21), 298 (20), 322 (14), 370 (8.0), 398 (4.3), 419 (3.5)	480	13.9	-2.50 d
<i>5meopy</i>	dpm	250 (31), 288 (22), 327(9.6), 358 (7.3), 384 (7.2), 426 (3.6), 450 (3.0)	525	13.3	-2.49 e
<i>bt</i>	dpm	216 (38), 258 (25), 321 (19), 340 (11), 379 (5.8), 401 (8.8), 443 (3.0)	530	7.7	-2.16
<i>pq</i>	dpm	250 (28), 298 (27), 325(8.8), 341 (8.8), 359 (9.3), 422 (6.8), 455 (3.6)	555	10.3	-2.00
<i>c6</i>	acac	300 (20), 388 (23), 469 (41), 496 (51)	590	54.1	-1.94
<i>dpo</i>	dpm	236 (24), 303 (27), 320 (22), 363 (10) 386 (8.8), 409 (6.7)	538	6.8	-2.40
<i>btp</i>	acac	265 (20), 318 (20), 344 sh (14), 427 (6.7), 444 (6.8)	600	11.3	-2.25
<i>thpy</i>	dpm	254 (13), 288 (17), 322 (15), 340 (17), 376 (8.2), 414 (4.6), 440 (4.6)	550	20.4	-2.41
<i>pyrpy</i>	dpm	237 (17), 300 (14), 331 (17), 354 (15), 370 (13), 460 (4.5), 487 (3.3)	580	16.1	-2.60 e
<i>bzq</i>	dpm	217 (38), 250 (36), 281 (9.3), 325 (11), 344 (9.0), 391 (5.8), 442 (2.4)	493	122	-2.22 e

a Absorption measurements of dpm complexes were carried out in hexanes; acac complexes were measured in CH_2Cl_2 . b 77 K emission and lifetime measurements were carried out in 2-methyltetrahydrofuran. c Redox measurements were carried out in DMF solution; values are reported relative to $\text{Cp}_2\text{Fe}/\text{Cp}_2\text{Fe}^+$. d Quasi-reversible. e Irreversible.

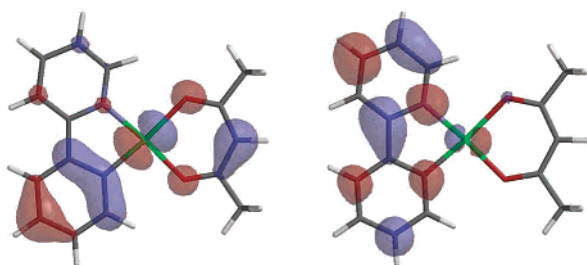


Figure 4. Density functional theory calculation (DFT) of HOMO (left) and LUMO (right) for *ppyPt(acac)*.

related cyclometalates and β -diketonate derivatives of Pt (vide supra). The HOMO and LUMO orbitals are shown in Figure 4. The HOMO and LUMO levels displayed in the figure have π symmetry, with opposite phases above and below the molecular plane. The HOMO (-5.41 eV) consists of a mixture of phenyl, Pt, and acac orbitals while the LUMO (-1.60 eV) is predominantly 2-phenylpyridyl in character. The triplet HSOMO (-2.64 eV) has a phase and spatial relation nearly identical to those of the singlet LUMO. The energy of the triplet state was estimated as the difference between the singlet ground state (HOMO) and triplet (HSOMO) energies. The theoretical triplet energy of 2.77 eV (448 nm) is comparable to lowest energy absorption band found for *ppyPt(dpm)* (2.88 eV, 430 nm) (vide infra). The valence orbital picture is consistent with combined LC and MLCT components in the lowest energy optical transition. The results of calculations for other $C^{\wedge}N$ Pt(acac) will be discussed in the following text as they apply to spectral interpretation.

Electrochemistry. The electrochemical properties of the complexes were examined using cyclic voltammetry, and the

redox data are given in Table 2. All of the electrochemical potentials reported here were measured relative to an internal ferrocene reference ($\text{Cp}_2\text{Fe}/\text{Cp}_2\text{Fe}^+$) or were adjusted to a ferrocene reference (for literature data only). Most complexes described here show a single reversible reduction wave between -1.9 and -2.6 V and irreversible oxidation. For example, *ppyPt(dpm)* has a reversible reduction wave at -2.41 V in DMF and an irreversible oxidation near 1.0 V. Similarly, the heteroleptic complex *ppyPt(en)* $^+$ is also reported to have a single reversible reduction wave at -2.6 V and an irreversible oxidation wave at $+0.51$ V in DMF solution. 22a Likewise, the $\text{Pt}(\text{ppy})_2$ complex is reported to have a reversible reduction at -2.5 V 39 and an irreversible oxidation at 0.1 V. Therefore, for these cyclometalated complexes, it is generally considered that reduction is localized on the $C^{\wedge}N$ ligand while oxidation occurs at the metal center. However, since square planar Pt(I) and Pt(III) metal centers are susceptible to nucleophilic attack by solvents, the Pt(II) redox processes are usually irreversible. 22a This electrochemical behavior is consistent with a description of ligand-localized LUMO states and a HOMO with substantial metal character, as seen in our DFT calculations. In addition, since Pt(II) complexes with *thpy* ligands have reversible reductions at the same potential as those with *ppy* ligands, it has been suggested that reduction occurs primarily on the more electron accepting pyridyl portion of the $C^{\wedge}N$ ligand. 40

Substituents on the 2-phenylpyridyl ligand strongly affect the redox properties of these complexes. Incorporating

(39) Cornioley-Deuschel, C.; von Zelewsky, A. *Inorg. Chem.* **1987**, *26*, 3354–3358.

(40) Kulikova, M. V.; Balashev, K. P.; Kvam, P.-I.; Songstad, J. *Russ. J. Gen. Chem.* **2000**, *70*, 163–170.

electron-withdrawing fluorine atoms on the phenyl ring gives a marked decrease in the reduction potential. The monofluorinated complex, *6fppyPt(dpm)*, has a reduction at -2.37 V, making it 40 mV easier to reduce than the *ppy* derivative, while the difluorinated derivatives, *46dfppyPt(dpm)* and *45dfppyPt(acac)*, are an additional 100 mV easier to reduce with reversible reduction waves at -2.31 and -2.27 V, respectively. Introduction of the weakly σ -donating methyl group on the pyridyl ring makes the *46dfp-4mepyPt(dpm)* complex 100 mV harder to reduce, relative to *46dfppyPt(dpm)*. Furthermore, substituting stronger electron-donating groups on the pyridyl ring, such as methoxy and dimethyl-amino, increases the reduction potential of *46dfp-4meopyPt(dpm)* to -2.51 V and *46dfp-4dmapyPt(dpm)* to -2.60 V. Similarly, substitution of electron-donating methoxy groups onto the phenyl ring leads to an equivalent cathodic shift. The *4meopyPt(dpm)* complex shows a quasi-reversible reduction potential at -2.50 V, and the *5meopyPt(dpm)* is irreversibly reduced at -2.49 V.

As the conjugated π system of the $C^{\wedge}N$ ligand is increased, complexes such as *btPt(dpm)*, *pqPt(dpm)*, and *btpPt(acac)* show a corresponding decrease in the reduction potential. For example, *pqPt(dpm)* has a reversible reduction wave at -2.00 V, and a second irreversible reduction is seen at -2.91 V. The decrease in reduction potential for these complexes is likely due to greater stabilization of the negative charge on the more delocalized π -orbital system. Interestingly, the *bzqPt(dpm)* complex is irreversibly reduced at -2.2 V. Similar behavior has been previously observed in related *bzqPtLX* systems and has been attributed to a weaker metal–ligand interaction due to the rigid planarity and enhanced conjugation of the benzoquinolyl ligand.⁴⁰

Electronic Spectroscopy. Absorption and low-temperature emission spectra were recorded for all of the complexes. The data are given in Table 2, and spectra for *ppyPt(dpm)*, *46dfppyPt(dpm)*, and *46dfp-4dmapyPt(dpm)* are shown in Figure 5. The *dpm* derivatives have nearly identical photo-physical properties (dilute solution and frozen glasses) as compared to their *acac* counterparts. The energies and extinction coefficients of these spectra are similar to those of other $C^{\wedge}N$ Pt complexes reported in the literature.^{20,22} Low-energy transitions in the range of 350–450 nm, with extinctions between 2000 and 6000 $M^{-1}cm^{-1}$, are assigned as metal-to-ligand charge transfer (MLCT) transitions. These bands are solvatochromatic⁴¹ and are not observed in the free $HC^{\wedge}N$ ligand precursors. The higher energy, more intense absorption bands are assigned to $\pi-\pi^*$ ligand-centered (LC) transitions. These transitions are shifted from the free ligand absorption due to perturbation from the metal, but are not strongly solvatochromic. Metal-centered, $d-d$, transitions are not observed for these complexes. It is believed that the

(41) *ppyPt(dpm)* is representative of the complexes examined here. The band at 381 nm in hexanes shifts to higher energies as the polarity of the solvent increases. This band comes at 374, 371, 366, and 360 nm in toluene, THF, acetone, and acetonitrile, respectively. The solvent polarity indexes for hexanes, toluene, THF, acetone, and acetonitrile are 0.1, 2.4, 4.0, 5.1, and 5.8, respectively. Polarity indexes were taken from the following: Snyder, L. R. *J. Chromatogr. Sci.* **1978**, *16*, 223–234. Snyder, L. R. *J. Chromatogr.* **1974**, *92*, 223–230.

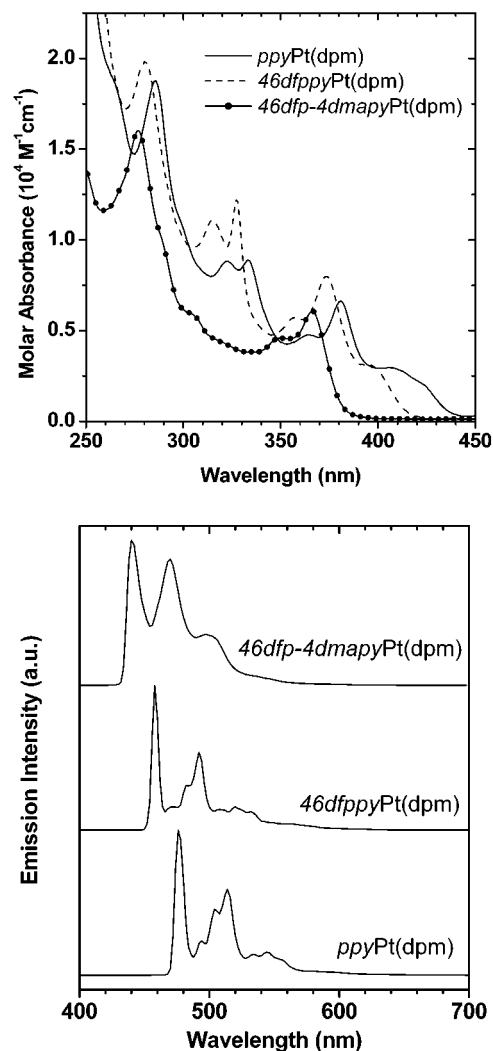


Figure 5. Absorption (top) and emission (bottom) spectra for *ppyPt(dpm)*, *46dfppyPt(dpm)*, and *46dfp-4dmapyPt(dpm)* complexes. The absorption spectra were measured in hexanes at room temperature, and the emission spectra were measured at 77 K in a 2-methyltetrahydrofuran glass.

strong ligand field of the $C^{\wedge}N$ ligands shifts the $d-d$ transitions to high energy, putting them under the more intense LC and MLCT transitions.^{20b,c}

All of the complexes are intensely emissive in low-temperature glasses (77 K), and many are luminescent in fluid solution (298 K) as well. Most of the complexes show a small rigidochromic blue shift of 5–10 nm on cooling of the solution sample to 77 K. The emission bands for all of the complexes are red-shifted from the phosphorescence of the corresponding protonated $C^{\wedge}N$ ligand and have shorter radiative lifetimes. For example, at 77 K, the emission maximum and lifetime of the *ppyPt(dpm)* complex ($\lambda_{max} = 480$ nm, $\tau = 9.0 \mu s$) can be compared to the phosphorescence emission maximum and lifetime of 2-phenylpyridine ($\lambda_{max} = 430$ nm, $\tau > 100$ ms).^{22b} The highly structured emission spectra display vibronic progressions of ca. $1400 cm^{-1}$, which are typical for breathing modes on the aromatic ring. The structured luminescence and microsecond radiative lifetimes at 77 K are consistent with emission originating from a mixed 3LC -MLCT excited state.^{23b} Longer lifetimes for some of the other complexes are indicative of greater 3LC character

in the excited state. The β -diketonato ligand does not significantly perturb the excited state since the luminescent properties of the *ppy* and *thpyPt(O^O)* complexes are comparable in wavelength, efficiency, and lifetime relative to *ppyPt(en)*⁺ and *thpyPt(en)*⁺ complexes reported in the literature.^{22a,c}

Substituent effects can be used to tune the energy of the emissive state for these *ppyPt*(β -diketonato) complexes over a wide range (Table 2). Incorporating an electronegative atom such as fluorine onto the phenyl ring hypsochromically shifts the emission spectrum. A single fluoride substituent in the 6'-position leads to a 12 nm blue shift in the emission of *6fppyPt(dpm)* ($\lambda_{\text{max}} = 468$ nm), relative to *ppyPt(dpm)*. Difluoro substitution at the 4',6'-positions on the phenyl ring gives a more pronounced blue shift in *46dfppyPt(dpm)* ($\lambda_{\text{max}} = 458$ nm). However, difluoro substitution at the 4',5'-positions causes a much smaller shift in *45dfppyPt(acac)* ($\lambda_{\text{max}} = 476$ nm). On the basis of the DFT calculations, it appears that a large amount of electron density in the HOMO is centered at the 5'-position of the phenyl ring and nodes exist at the 4'- and 6'-positions (the HOMO orbitals for difluoro-*ppyPt* complexes look very similar to the one shown for *ppyPt(acac)* in Figure 4). Therefore, for *45dfppyPt(acac)*, weak π donation into this molecular orbital from the 5'-fluoro group raises the HOMO level and offsets the electron-withdrawing effect from the 4'-fluoro group. Similarly, substitution with a more strongly electron donating methoxy group in the 5'-position gives a pronounced red shift in *5meoppyPt(dpm)* ($\lambda_{\text{max}} = 525$ nm) relative to the 4'-position in *4meoppyPt(dpm)* ($\lambda_{\text{max}} = 480$ nm). This sensitivity of transition energy to the substitution position on 2-phenylpyridyl ligands has been previously observed in related tris-cyclometalated iridium complexes.⁴²

In order to further increase the energy gap of the emitting excited state, electron-donating groups were incorporated onto the pyridyl ring since substitution on this ring should raise the LUMO energy and thereby increase the HOMO–LUMO energy gap. Consistent with this argument, methyl and dimethylamino donors in the 4-position of the respective pyridyl rings of *46dpf-4mepyPt(dpm)* and *46dpf-4dmapyPt(dpm)* clearly increase the reduction potential relative to *46dpfppyPt(dpm)* (vide supra). Consequently, the lowest energy MLCT absorption bands for the *46dfppy*, *46dfp-4mepy*, and *46dfp-4dmapy Pt(dpm)* complexes decrease in series 394, 390, and 365 nm, respectively. Higher energy $\pi-\pi^*$ transitions between 250 and 300 nm are not as strongly perturbed, but also show hypsochromic shifts in wavelength such that *46dfppy* > *46dfp-4mepy* > *46dfp-4dmapy*. A similar trend is seen in the emission spectra; a weakly σ -donating methyl group in the 4-position on the pyridyl ring results in a slight blue shift of 2 nm for *46dfp-4mepyPt(dpm)* ($\lambda_{\text{max}} = 456$ nm) while the stronger dimethylamino donor imparts a more substantial shift for *46dfp-4dmapyPt(dpm)* ($\lambda_{\text{max}} = 440$ nm).

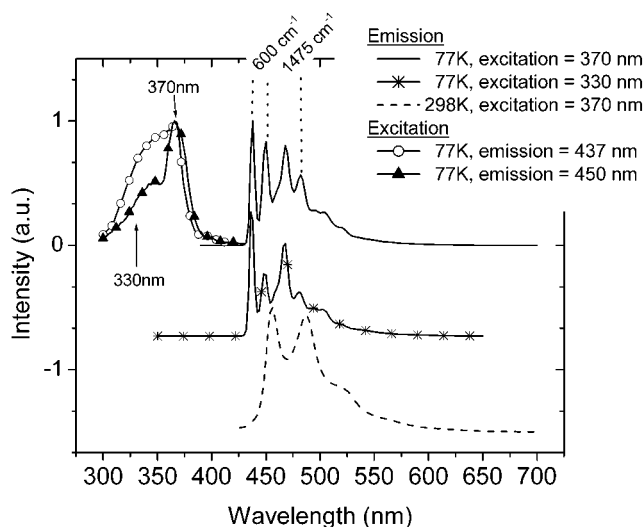


Figure 6. Room temperature and 77 K emission and excitation spectra for *46dfp-4meopyPt(acac)* in 2-methyltetrahydrofuran solution.

The emission characteristics of the methoxy-substituted complexes display some distinct features that require separate consideration. A comparison of the room temperature and 77 K emission spectra for *46dfp-4meopyPt(acac)* in 2-MeTHF is shown in Figure 6. At room temperature the structured spectrum has a maximum at 456 nm with a vibronic spacing of 1400 cm^{-1} . Interestingly, at 77 K the luminescence spectrum displays two emission bands as separate vibronic progressions (1475 cm^{-1}) separated by 600 cm^{-1} . The intensity of the higher energy progression is greatly attenuated in 3-methylpentane glass at 77 K. The same emissive behavior is observed with the dpm derivative (i.e., *46dfp-4meopyPt(dpm)*) in 2-MeTHF. A similar effect is also observed for the *5meoppyPt(dpm)* complex in which two sets of vibronic progressions are observed. These two progressions are also separated from each other by roughly 600 cm^{-1} with the higher energy transition of much lower intensity. While the spectra could be explained as being due to two vibronic progressions (600 and 1450 cm^{-1}) on a single electronic transition, the excitation and emission spectra suggest that this is not the case. The excitation spectra for the two different progressions ($\lambda_{\text{max}} = 437$ and 450 nm) are different, and the ratio of the higher energy to the lower energy progression is strongly affected by the excitation wavelength (Figure 6). Had the spectral line shape been caused by two vibronic progressions on a single electronic transition, the ratio of the two progressions should not depend on the excitation energy, which they clearly do. The best explanation for the low-temperature spectra of this complex is the appearance of two different emitting species in the low-temperature glass. All of the methoxy derivatives were carefully examined by NMR spectroscopy and found to consist of a single species. This analysis is further substantiated by the fact that the ratio of the two states is dependent on the coordinating nature of the solvent, as seen from the differences in emission for 3-methylpentane and 2-methyltetrahydrofuran solutions. The source of the two emitting species is unknown at present but could be due to confor-

(42) (a) Dedeian, K.; Djurovich, P. I.; Garces, F. O.; Carlson, G.; Watts, R. J. *Inorg. Chem.* **1991**, *30*, 1685–1687. (b) Grushin, V. V.; Herron, N.; LeCloux, D. D.; Marshall, W. J.; Petrov, V. A.; Wang, Y. *Chem. Commun.* **2001**, 1494–1495.

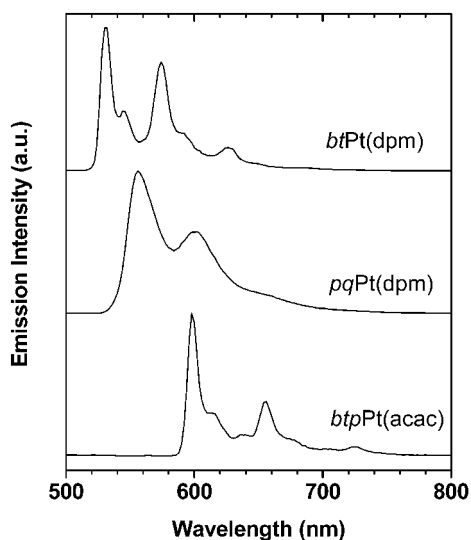


Figure 7. 77 K emission spectra for *btPt(dpm)*, *pqPt(dpm)*, and *btpPt(acac)* complexes in 2-methyltetrahydrofuran.

mational isomerism of the methoxy group with respect to the pyridyl ring.

The nature of the $C^{\wedge}N$ ring system can also have profound effects on the color of emission. Complexes with softer, more polarizable atoms such as sulfur and nitrogen incorporated in the ring system are much easier to oxidize and have significantly lower transition energies. Therefore, the *thpyPt(dpm)* and *pyrpyPt(dpm)* complexes display orange-red emission with a λ_{\max} up to 600 nm. Extending the size of the conjugated π system for $C^{\wedge}N$ ligands compared to 2-phenylpyridyl expectedly lowers the energy of the 3LC transition by simultaneously raising the HOMO and lowering the LUMO energy. Thus, the complexes *btPt(dpm)*, *pqPt(dpm)*, and *btpPt(acac)* emit yellow to red compared to the green of *ppyPt(dpm)* (Figure 7). The *bzqPt(dpm)* complex is unique because of its exceptionally long lifetime of 120 μ s in 77 K solution. A similar long lifetime for the related *bzqPt(en)*⁺ complex ($\tau = 217 \mu$ s at 77 K)⁴⁰ has been attributed to the increased conjugation within the ligand π system due to the rigid planarity of the benzoquinolyl chelate. This leads to both a decrease in the energy of the 3LC excited state and a weaker metal–ligand interaction, thus increasing the 3LC character of the excited state.

The compounds *dpo* and *c6* are commercially available laser dyes with fluorescence maxima at 365 and 500 nm, respectively. It has been recently demonstrated that these dyes can cyclometalate onto iridium.^{9a} Laser dyes, in general, have very high extinction coefficients and fluoresce very efficiently, whereas emission from the triplet state may only be observed at low temperature, if at all. However, the Ir cyclometalated dyes only display emission from ligand-centered triplet states. Likewise, the *dpoPt(dpm)* and *c6Pt(acac)* complexes emit exclusively from triplet excited states (*dpoPt(dpm)*, $\lambda_{\max} = 538$ nm, $\tau = 6.8 \mu$ s; *c6Pt(acac)*, $\lambda_{\max} = 590$ nm, $\tau = 28 \mu$ s). Hence, cyclometalating a laser dye to the heavy Pt metal atom also allows for facile intersystem crossing between the singlet and triplet manifolds of the dye.

Many of these complexes are also highly emissive in degassed room temperature solution with lifetimes in the

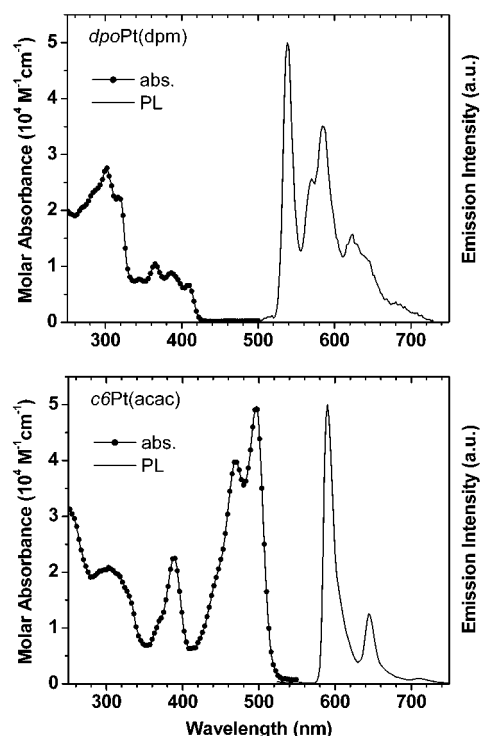


Figure 8. Absorption and emission spectra for *dpoPt(dpm)* (top) and *c6Pt(acac)* (bottom) complexes. The absorption spectrum of *dpoPt(dpm)* was measured in hexanes, and *c6Pt(acac)* in CH_2Cl_2 , both at room temperature. The emission spectra were measured at 77 K in a 2-methyltetrahydrofuran glass.

Table 3. Emission Properties of $C^{\wedge}NPt(O^{\wedge}O)$ Complexes at Room Temperature^a

$C^{\wedge}N$	$O^{\wedge}O$	λ_{\max} , nm	τ_{298} , μ s	Φ_{PL}
<i>ppy</i>	<i>acac</i>	486	2.6	0.15
<i>p-tpy</i>	<i>acac</i>	485	4.5	0.22
<i>6fp</i>	<i>dpm</i>	476	<1.0	0.06
<i>46dfppy</i>	<i>acac</i>	484	3.0	0.22
<i>46dfppy</i>	<i>acac</i>	466	<1.0	0.02
<i>46dfppy</i>	<i>dpm</i>	466	<1.0	0.02
<i>46dfp-5mepy</i>	<i>dpm</i>	472	<1.0	0.05
<i>46dfp-4meopy</i>	<i>dpm</i>	456	<1.0	
<i>46dfp-4dmapy</i>	<i>dpm</i>	447	<1.0	
<i>4meopy</i>	<i>dpm</i>	490	7.4	0.20
<i>c6</i>	<i>acac</i>	589	27.9	0.25
<i>btp</i>	<i>acac</i>	612	3.4	0.08
<i>thpy</i>	<i>acac</i>	575	4.5	0.11
<i>pyrpy</i>	<i>acac</i>	603	7.14	0.02

^a 2-Methyltetrahydrofuran solutions.

microsecond regime; data for several of the complexes is shown in Table 3. As the energy of emission increases, a corresponding decrease in room temperature quantum efficiency and lifetime is observed. The luminescent quantum yield of the *ppy* complex is 15% ($\tau = 2.6 \mu$ s), whereas the *46dfppy* complex has a quantum yield of only 2% ($\tau < 2 \mu$ s) and the quantum yields of the *46dfp-4meopy* and *46dfp-4dmapy* complexes are <0.1%. It appears that a new luminescent quenching mechanism comes into play as the energy of the 3LC excited state increases. The nature of this process is unknown at this time, but may involve a self-quenching mechanism or perhaps thermal activation to either a MC state or a competing MLCT state on the ancillary β -diketonato ligand. Further work is underway in order to elucidate the origin of this phenomenon.

Conclusions

The different $C^N Pt(O^O)$ complexes presented here demonstrate that these complexes can be readily tuned to emit with high efficiency throughout the visible spectrum. The emission characteristics of these complexes are governed by the nature of the cyclometalating ligand, C^N , with the spectra resembling the ligand phosphorescence spectra. Strong spin-orbit coupling of the heavy platinum atom allows for mixing of 1MLCT with ligand-based $^3\pi-\pi^*$, making the formally forbidden radiative relaxation of these states an efficient process, with quantum efficiencies as high as 0.25 at room temperature. All of these complexes are strongly emissive in the solid state and at 77 K with lifetimes on the order of microseconds. Many of these complexes are also emissive in fluid solution. These complexes are easily prepared, neutral, stable in air, and sublimable, making them good candidates for use in optoelectronic devices. The wide range of excited state energies and redox potentials reported here make this series of Pt complexes attractive as highly tunable photooxidants and photoreductants.

We have recently incorporated one of these Pt complexes into an organic light emitting diode, which emitted white light very efficiently (Q.E. = 4% (photons/electrons)).⁴³ We are currently examining a range of Pt complexes for both monochrome and white OLEDs. These results of these studies will be reported in future publications.

Acknowledgment. The authors thank Universal Display Corp., the Defense Advanced Research Projects Agency, and the National Science Foundation for financial support of this work. We would also like to thank Dr. Stephen Bradforth and Amy Germaine for helpful discussions.

Supporting Information Available: Crystal data, atomic coordinates, bond distances, bond angles, anisotropic displacement parameters, and ORTEP diagrams for *thpyPt(dpm)*. This material is available free of charge via the Internet at <http://pubs.acs.org>.

IC0255508

(43) D'Andrade, B. W.; Brooks, J.; Adamovich, V.; Thompson, M. E.; Forrest, S. R. *Adv. Mater.*, in press.